Determining urban material activities with a vehicle-based multi-sensor system

Marco Salathe

Applied Nuclear Physics Program

5 October 2021

Gamma-ray detection for homeland security

- Goal: detect radioactive sources outside of regulatory control
- Problem: high variability of naturally occurring radioactive materials (NORMs) reduce system sensitivity
- Our approach here: Model radioactive background with contextual sensor data
  - Focus on a simple urban mock facility with known radioisotope composition
  - Build a three dimensional model of the surrounding that includes the most crucial features
  - Include energy-dependence though modeling radioisotope spectrum, providing access to activities
  - MLEM to attribute radiological measurements to surroundings

Street scale: Portable devices and stationary devices

Block scale: Mobile devices (truck, car, drones)

City scale: Airborne devices (helicopter) and detector networks

Gamma-ray detection for homeland security

- Goal: detect radioactive sources outside of regulatory control
- Problem: high variability of naturally occurring radioactive materials (NORMs) reduce system sensitivity
- Our approach here: Model radioactive background with contextual sensor data
  - Focus on a simple urban mock facility with known radioisotope composition
  - Build a three dimensional model of the surrounding that includes the most crucial features
  - Include energy-dependence though modeling radioisotope spectrum, providing access to activities
  - MLEM to attribute radiological measurements to surroundings

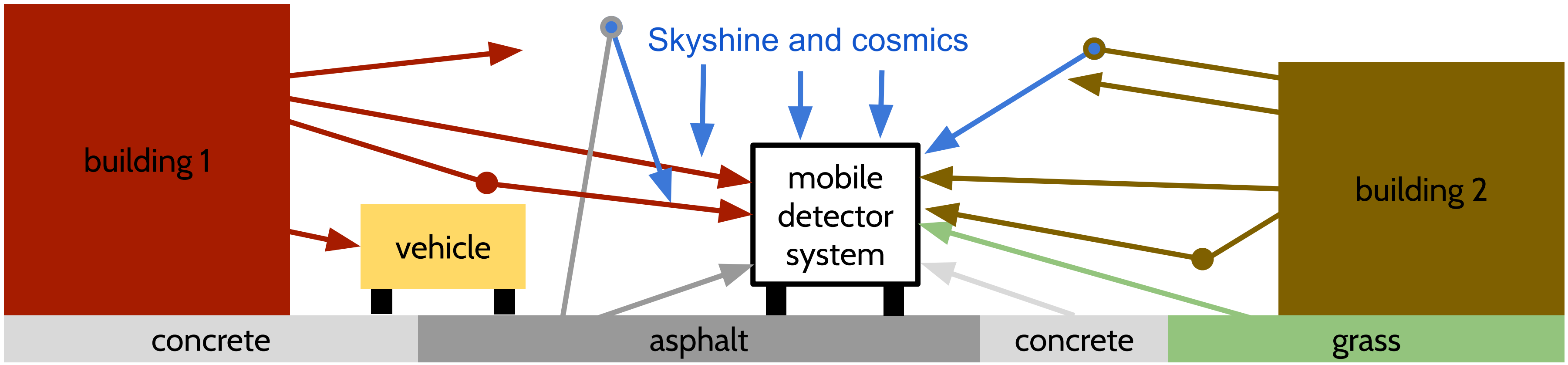

Gamma-ray detection for homeland security

- Goal: detect radioactive sources outside of regulatory control
- Problem: high variability of naturally occurring radioactive materials (NORMs) reduce system sensitivity
- Our approach here: Model radioactive background with contextual sensor data
    - Focus on a simple urban mock facility with known radioisotope composition
    - Build a three dimensional model of the surrounding that includes the most crucial features
    - Include energy-dependence though modeling radioisotope spectrum, providing access to activities
    - MLEM to attribute radiological measurements to surroundings

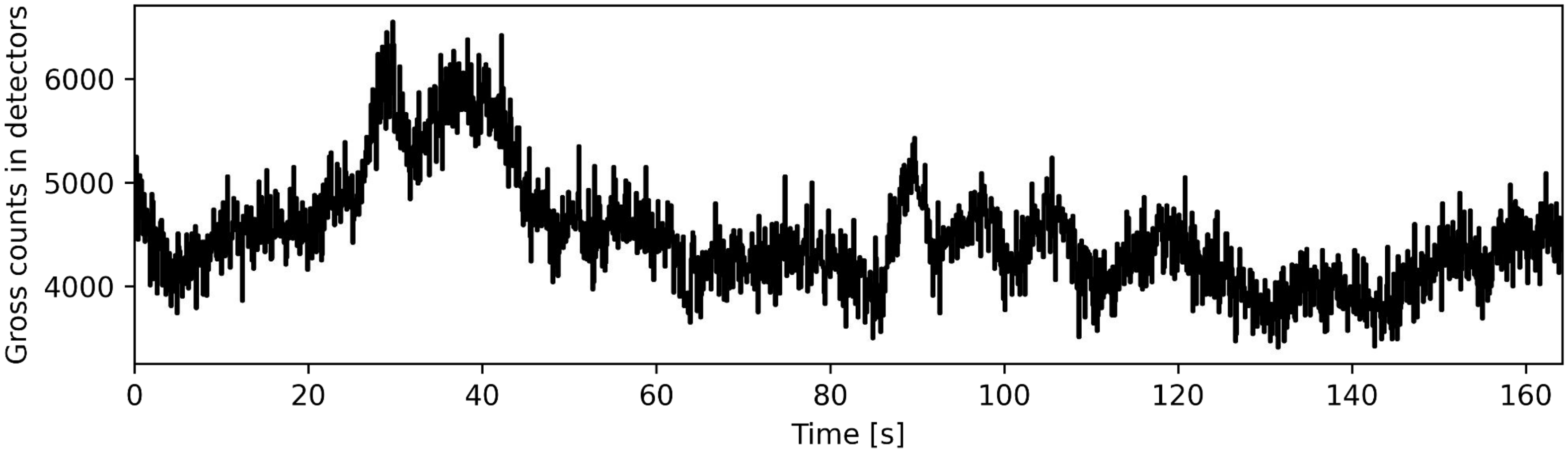

BERKELEY LAB

Gamma-ray detection for homeland security

- Goal: detect radioactive sources outside of regulatory control
- Problem: high variability of naturally occurring radioactive materials (NORMs) reduce system sensitivity
- Our approach here: Model radioactive background with contextual sensor data
  - Focus on a simple urban mock facility with known radioisotope composition
  - Build a three dimensional model of the surrounding that includes the most crucial features
  - Include energy-dependence though modeling radioisotope spectrum, providing access to activities
  - MLEM to attribute radiological measurements to surroundings

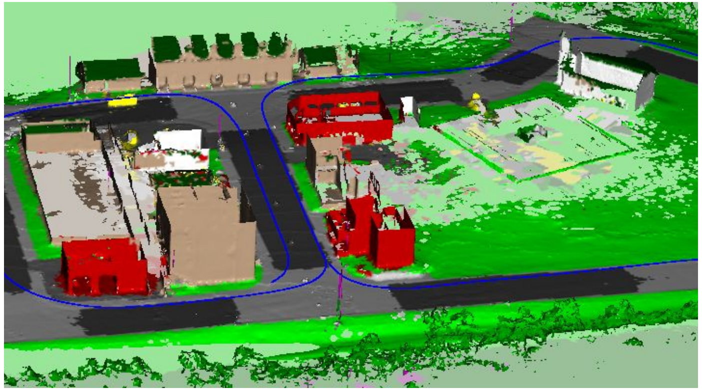

Linear system:

$$\boldsymbol{\lambda} = \boldsymbol{R}\boldsymbol{f}$$

Maximum Likelihood Maximization Estimation for solving system

Radiological Multi-sensor Analysis Platform (RadMAP)

- 100 NaI(Tl) detectors in a coded mask array
- NovAtel SPAN-CPT GPS/INS receiver
- 2x Velodyne HDL-32E LiDAR units
- 2x Point Grey Ladybug 3 cameras (360 deg view)
- Additional sensors and detectors not used for this analysis

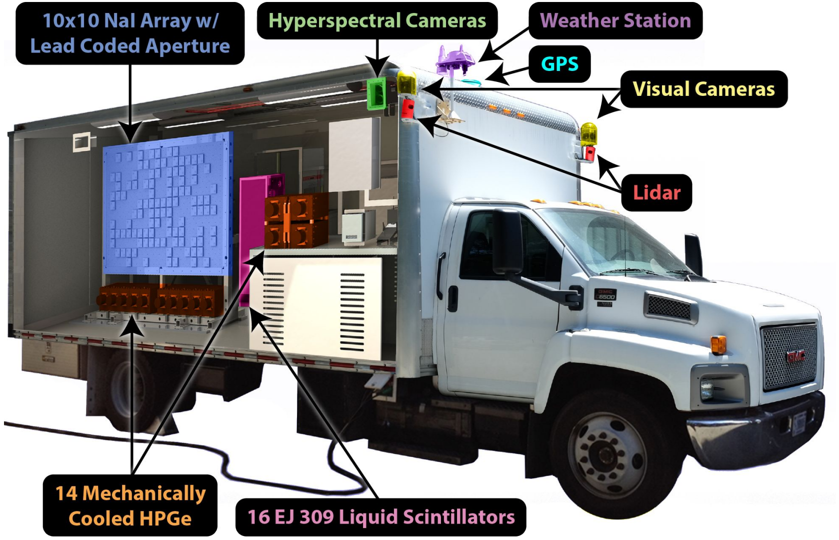

Bandstra et al., "RadMAP: The Radiological Multi-sensor Analysis Platform", NIM A, 840: 59–68 (2016)

RadMAP campaign at FtIG (Pennsylvania)

- Military Operations in Urban Terrain facility at the Fort Indiantown Gap (FtIG) National Guard Base
- RadMAP was brought to FtIG as part of the Multiagency Urban Search Experiment (MUSE) collaboration in 2016
    - Dataset considered for this study is a 164s drive around the facility
    - Only using NaI radiation data

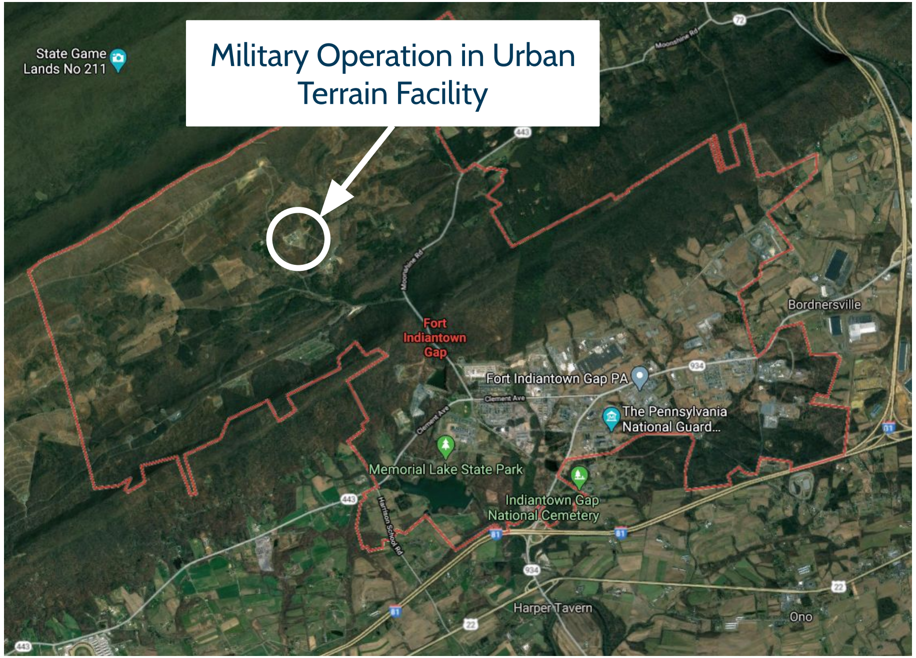

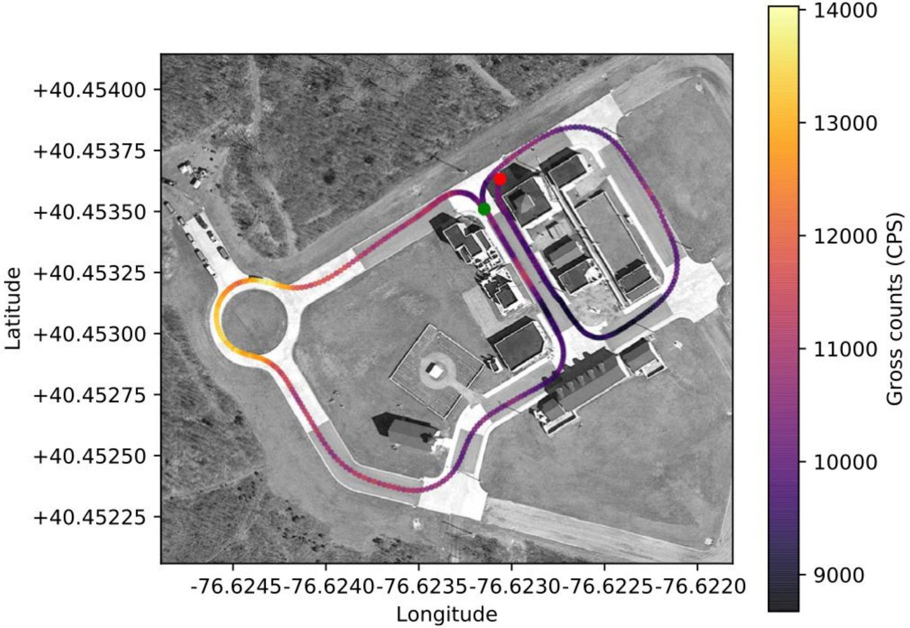

D.E. Archer et al., Modeling Urban Scenarios & Experiments: Fort Indiantown Gap Data Collections Summary and Analysis. United States, 2017.

NORM measurements at FtIG

- A set of naturally occurring radioactive materials at the Military Operations in Urban Terrain facility have been characterized by collaborators
- Mechanically cooled HPGe detectors in lead caves open on face exposed to surface
- 70 measurements (~30min each) of asphalt, soil, walls, sidewalk and gravel at various locations

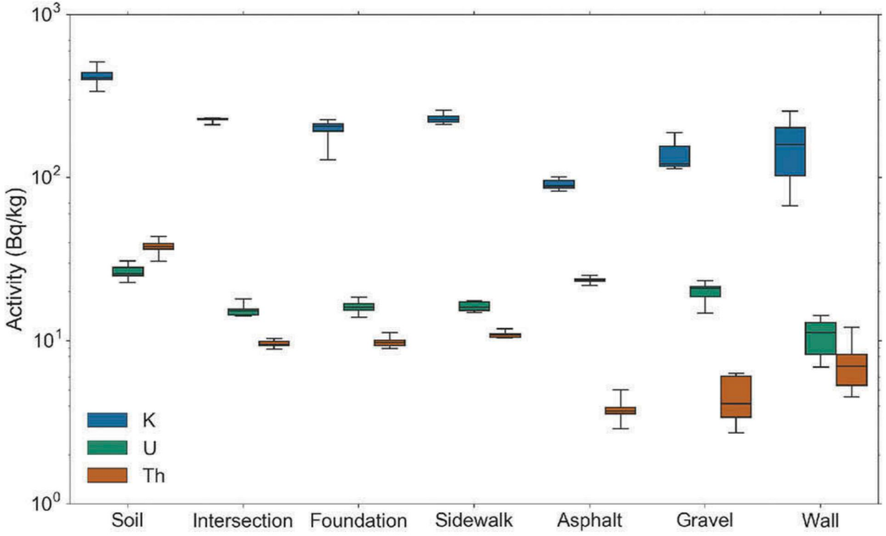

M. W. Swinney, et al., A methodology for determining the concentration of naturally occurring radioactive materials in an urban environment. Nuclear Technology, 203(3):325-335, 2018.

Modeling Gamma-ray backgrounds

- Various gamma-ray emission of from surfaces (NORM)
  - Terrestrial — K-40, U-238 series, Th-232 series (KUT)
  - Airborne — radon, skyshine
  - Cosmic — continuum, 511 keV from positrons
- Inversion problem
  - Predict radiation and it's transport by classifying visible surfaces as seen from the detector system
  - Build a system of linear equations (system response) to solve for the unknown gamma-ray flux from various surfaces
- System response
  - 3D description of the facility (distance and material class)
  - Effective area (detector efficiency and geometry) and description of gamma-ray transport in air
  - NORM modelling for complexity reduction originating from energy dependence of radiological data

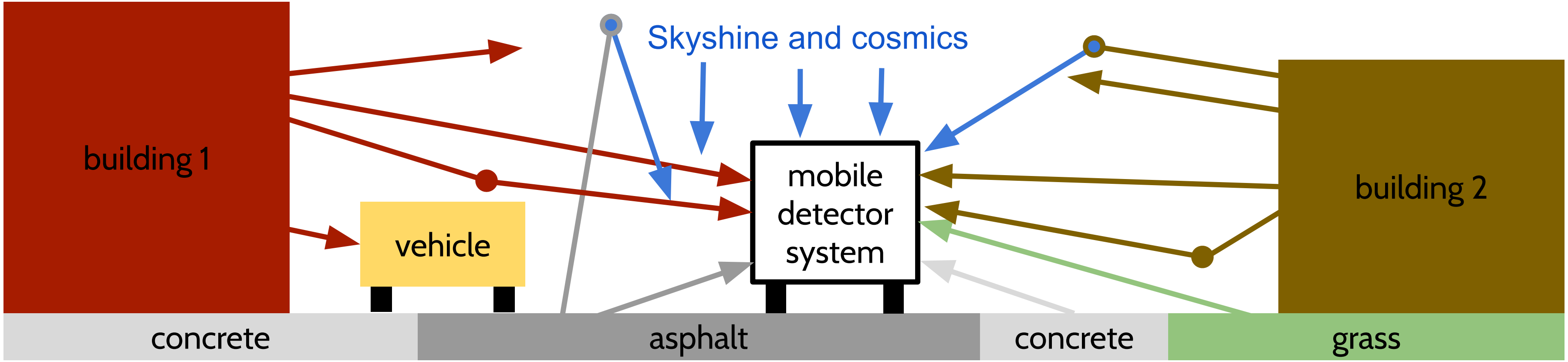

Modeling Gamma-ray backgrounds

- Various gamma-ray emission of from surfaces (NORM)
  - Terrestrial — K-40, U-238 series, Th-232 series (KUT)
  - Airborne — radon, skyshine
  - Cosmic — continuum, 511 keV from positrons
- Inversion problem
  - Predict radiation and it's transport by classifying visible surfaces as seen from the detector system
  - Build a system of linear equations (system response) to solve for the unknown gamma-ray flux from various surfaces
- System response
  - 3D description of the facility (distance and material class)
  - Effective area (detector efficiency and geometry) and description of gamma-ray transport in air
  - NORM modelling for complexity reduction originating from energy dependence of radiological data

M. S. Bandstra, et al., Attribution of gamma-ray background collected by a mobile detector system to its surroundings using panoramic video, NIMA 954, 161126, 2020.

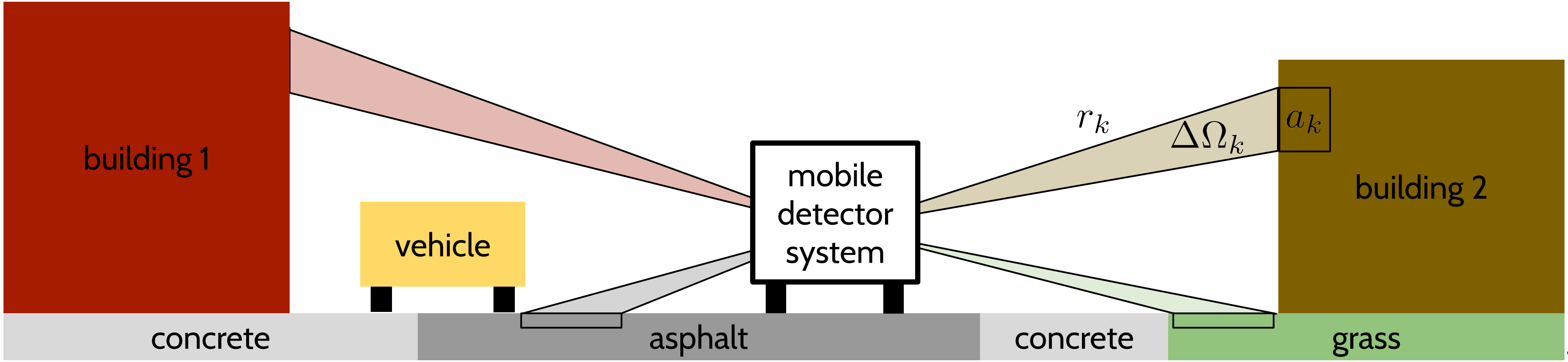

Modeling Gamma-ray backgrounds

- Various gamma-ray emission of from surfaces (NORM)
  - Terrestrial — K-40, U-238 series, Th-232 series (KUT)
  - Airborne — radon, skyshine
  - Cosmic — continuum, 511 keV from positrons
- Inversion problem
  - Predict radiation and it's transport by classifying visible surfaces as seen from the detector system
  - Build a system of linear equations (system response) to solve for the unknown gamma-ray flux from various surfaces
- System response
  - 3D description of the facility (distance and material class)
  - Effective area (detector efficiency and geometry) and description of gamma-ray transport in air
  - NORM modelling for complexity reduction originating from energy dependence of radiological data

M. S. Bandstra, et al., Attribution of gamma-ray background collected by a mobile detector system to its surroundings using panoramic video, NIMA 954, 161126, 2020.

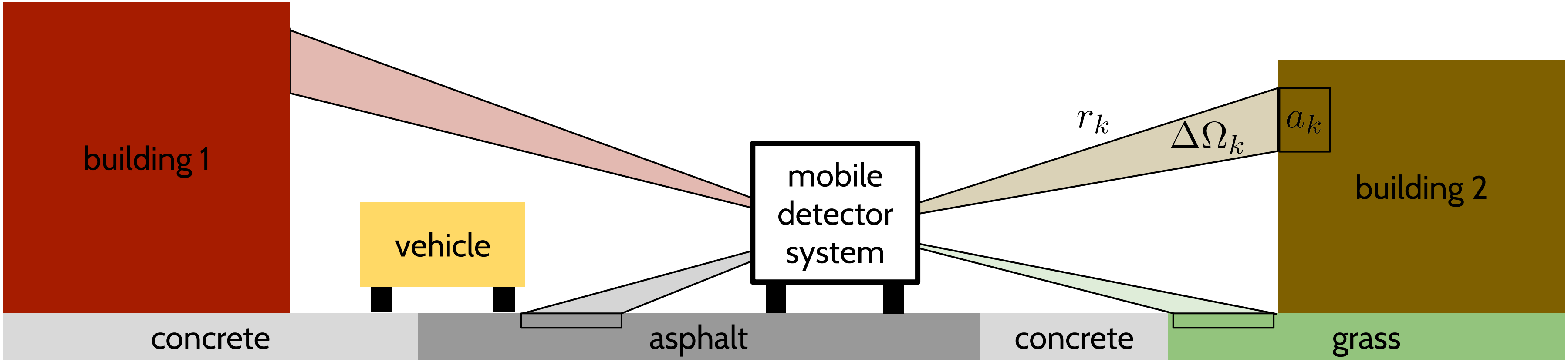

Building a 3D description of the facility

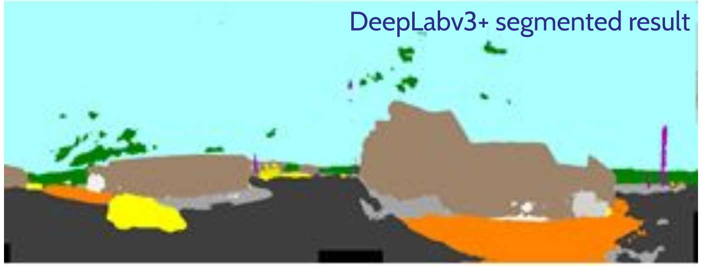

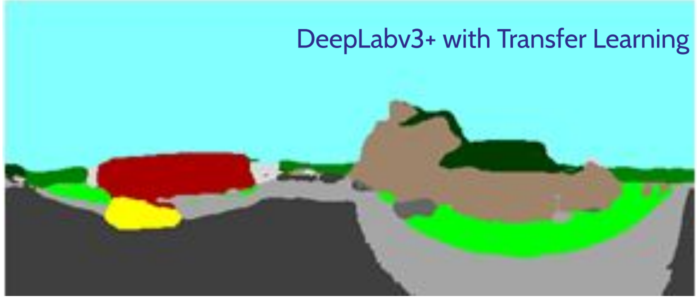

Segmentation and classification of images

- Used Google's Deep Labelling for Semantic Image Segmentation (DeepLabv3+) model on pre-trained Cityscapes[1] dataset

- Applied transfer learning by retraining last, fully-connected neural layer with 45 hand-labeled images to be closer to ground truth labels:
  - *Asphalt*
  - *Building red*
  - *Building brown*
  - *Building white*
  - *Building roof*
  - *Concrete*
  - *Forest*
  - *Grass*
  - *Gravel*
  - *Sky*
  - *Vehicle*

[1]*Cityscapes dataset available at: https://www.cityscapes-dataset.com*

[2]*L.Chen, et. al., Encoder-Decoder with Atrous Separable Convolution for Semantic Image Segmentation, ECCV, 2018, https://github.com/tensorflow/models/tree/master/research/deeplab*

Building a 3D description of the facility

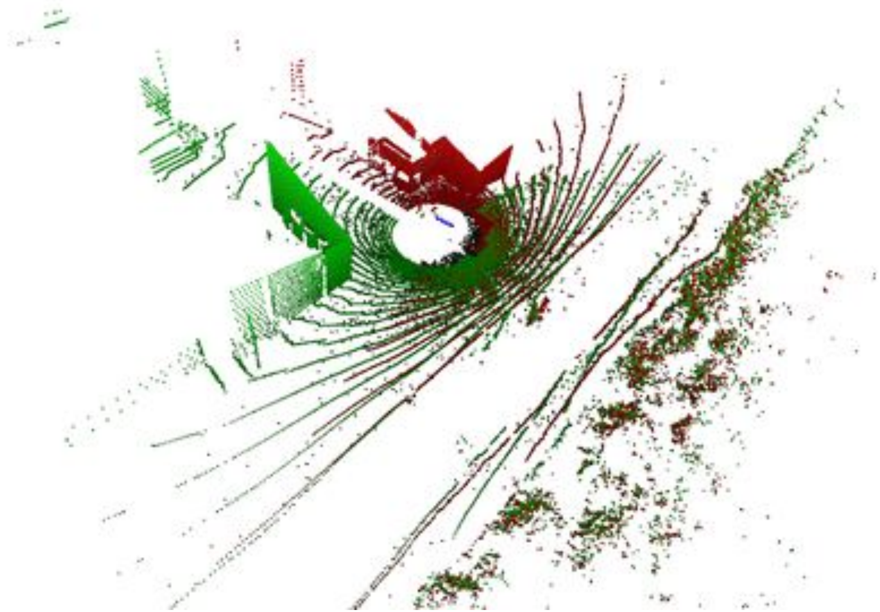

Assemble LiDAR data to a model (SLAM)

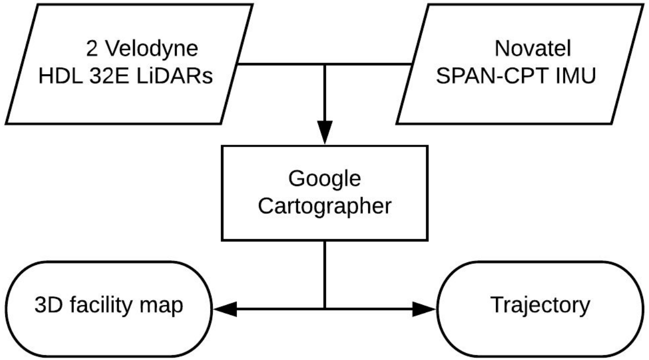

- Simultaneous Localization and Mapping (SLAM) using Google Cartographer
- Minimize cost function between current LiDAR data and the reconstructed map from previous data
- Rotation frequency of LiDAR 10Hz

W. Hess, D. Kohler, H. Rapp, and D. Andor, Real-Time Loop Closure in 2D LIDAR SLAM, International Conference on Robotics and Automation (ICRA), IEEE, 2016, https://github.com/googlecartographer/cartographer

Building a 3D description of the facility

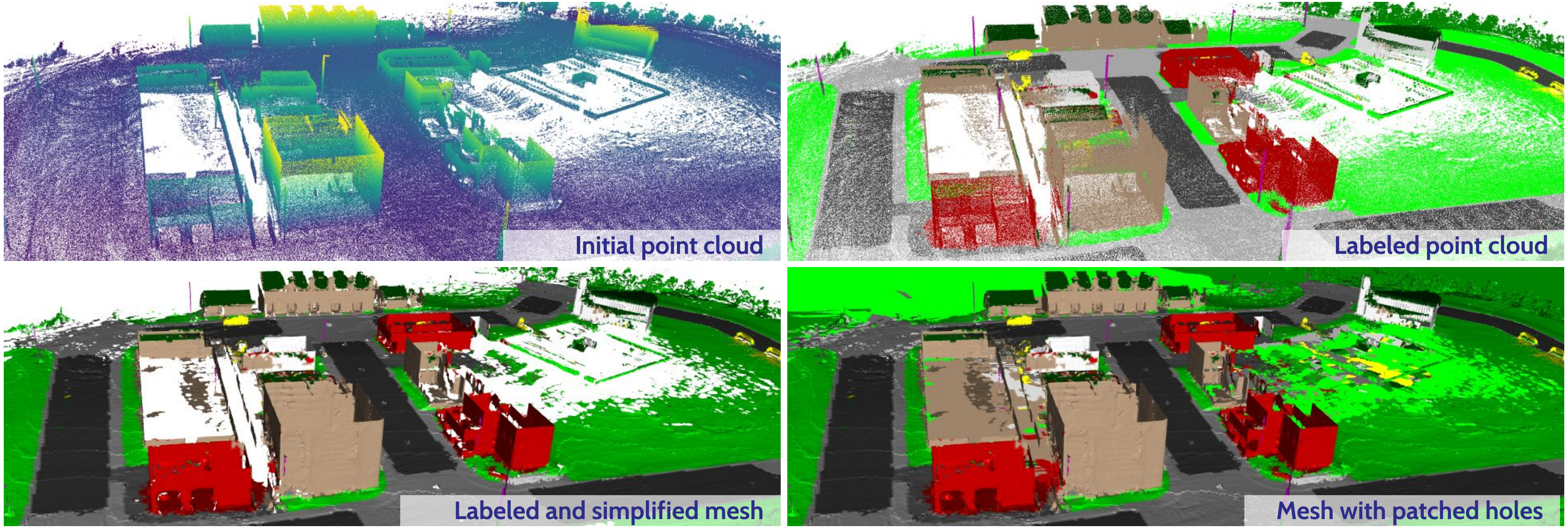

Convert Point Cloud to Labeled Mesh

- Projecting labeled images back to point cloud and pick the label that is observed most often at each point.
- Convert labeled point cloud into a triangular mesh (based on ball pivoting algorithm with smart normal orientation algorithm)
  - Implementation of Hidden Point Removal Operator[1] into Open3D[2]
- Simplify mesh to reduce number of vertices by a factor of ~10
- Remaining holes are patched using nearest neighbor interpolation and extending to a flat horizon

[1] *S. Katz, A.Tal, and R. Basri, Direct visibility of point sets, ACM Trans, Graph. 26, 3, Article 24, 2007*

[2] *Q. Zhou, J. Park, V. Koltun, Open3D: A Modern Library for 3D Data Processing, arXiv:1801.09847, 2018, http://www.open3d.org*

Building a 3D description of the facility

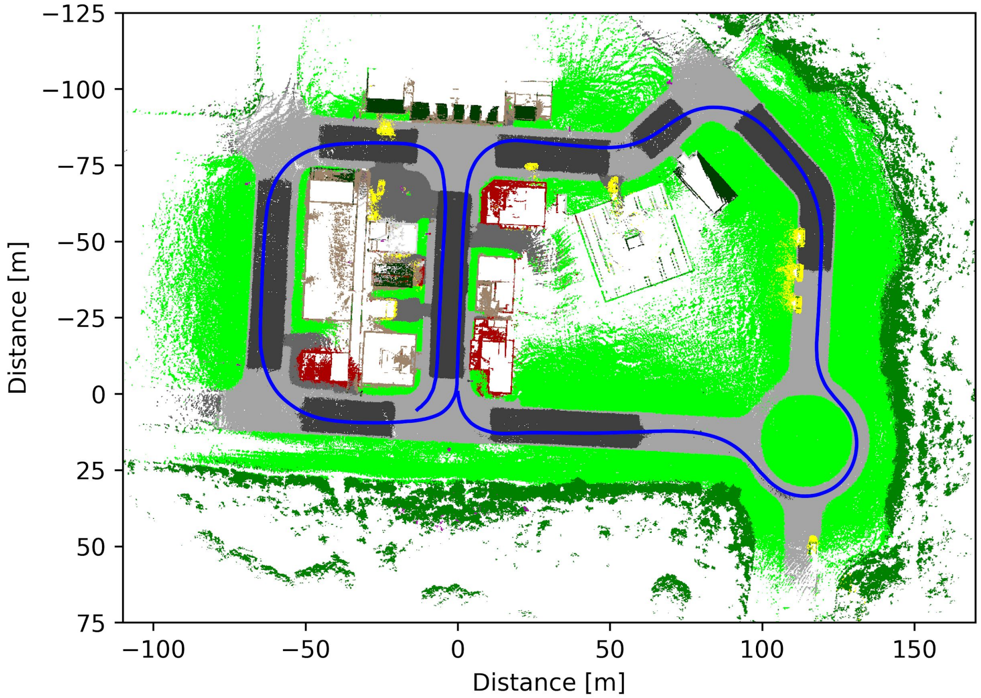

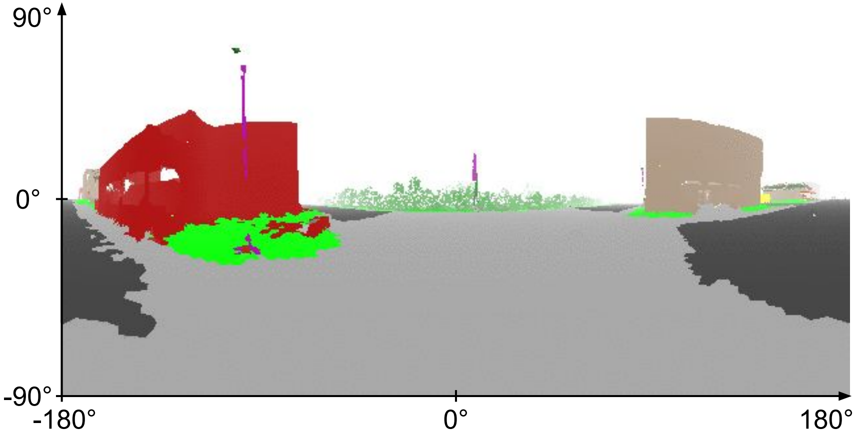

- The distance and material class of all the surfaces in the field of view of each detector can be calculated at every time step
- Visualization of panoramic view of mesh from detector array center
- Alpha channel is distance between 0 (transparent) and 80 meter (white)

Detector response (Effective Area)

- Effective area A_i is product of efficiency and geometric area
- Simulated using a simple model of RadMAP in all 4π
- Folded with estimated detector energy resolution

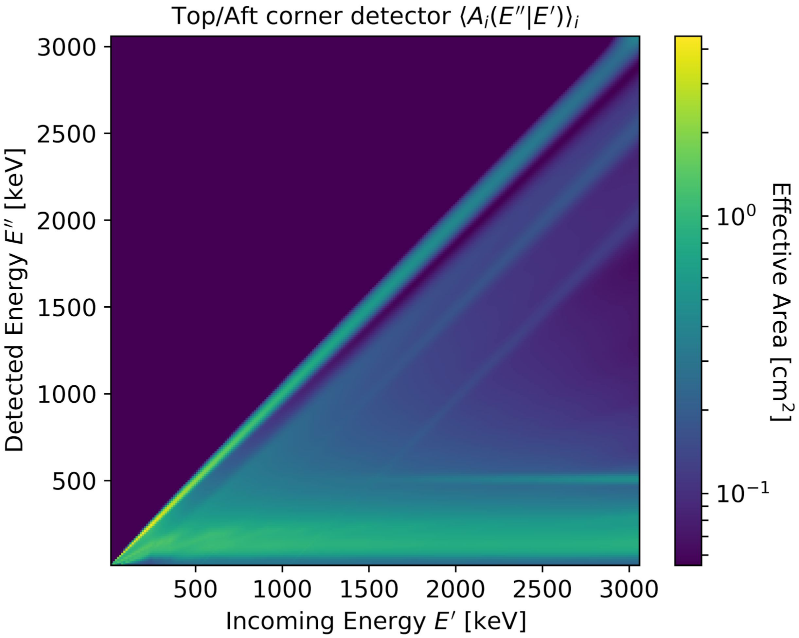

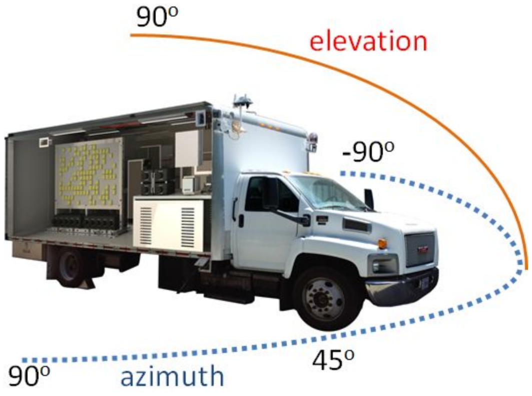

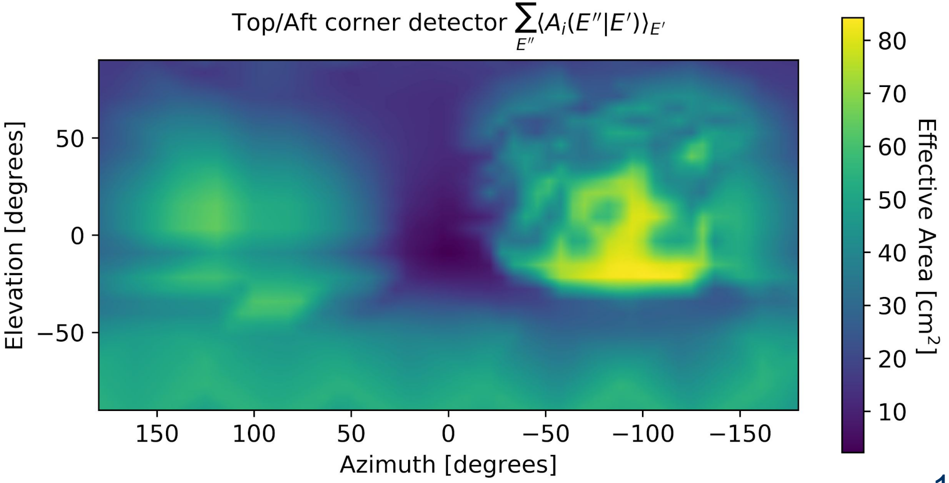

Down scattering in air

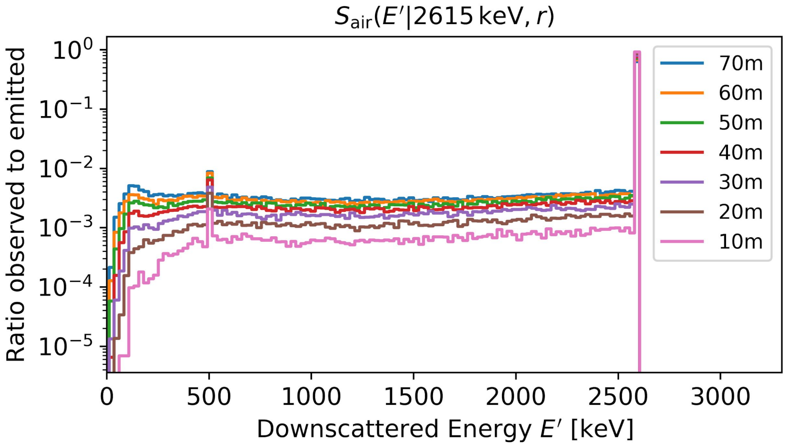

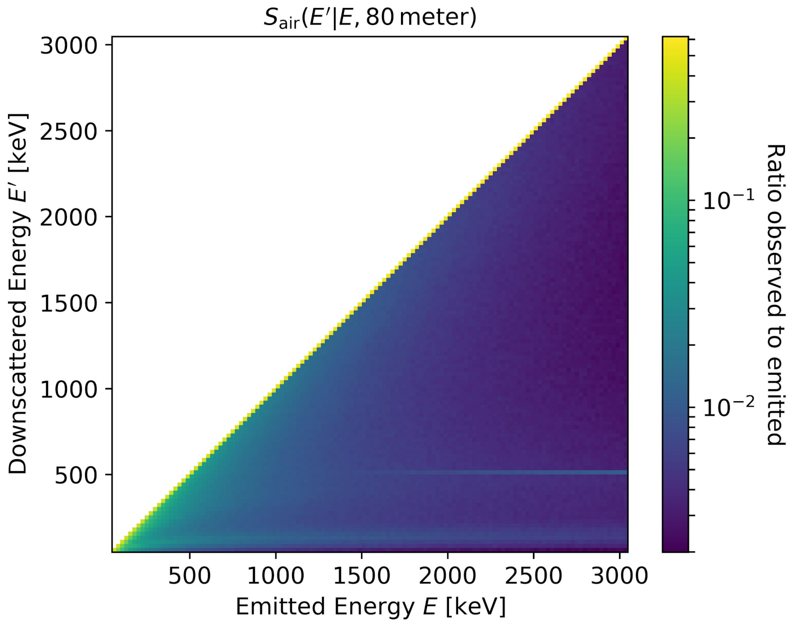

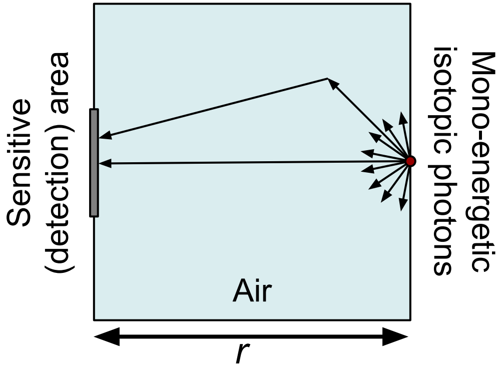

- Down scattering in air has been simulated with a tool developed by Mark S. Bandstra named *Ersatz* (not yet published)
  - A square box with equal sides was used as a simulation volume
  - Gamma-rays were emitted isotropically from a point-like mono-energetic source
  - The sensitive (detection) area covered 1/9th of the surface opposing the source

Complexity reduction with NORM modeling

Main sources of NORM:

- Terrestrial (KUT)
  - K-40,
  - U-238 series,
  - Th-232 series
- Airborne
  - Radon
  - skyshine
- Cosmic
  - Continuum
  - 511 keV from positrons

- K, U and T from simulation, leaving 3 free parameters for each label
- Modeling airborne and cosmic is hard, energy dependence was not enforced (~120 free parameters)
- About 155 free parameters in total, a factor of 10 improvement from an unconstrained fit

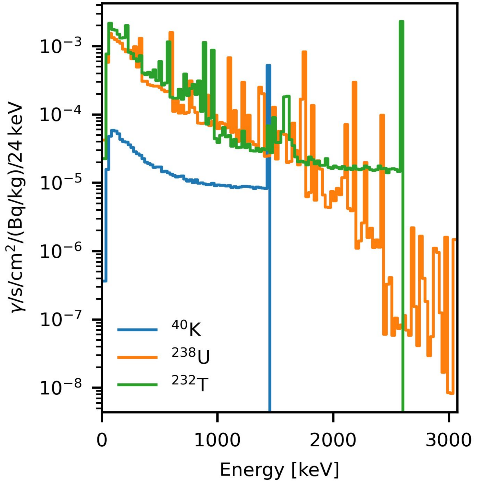

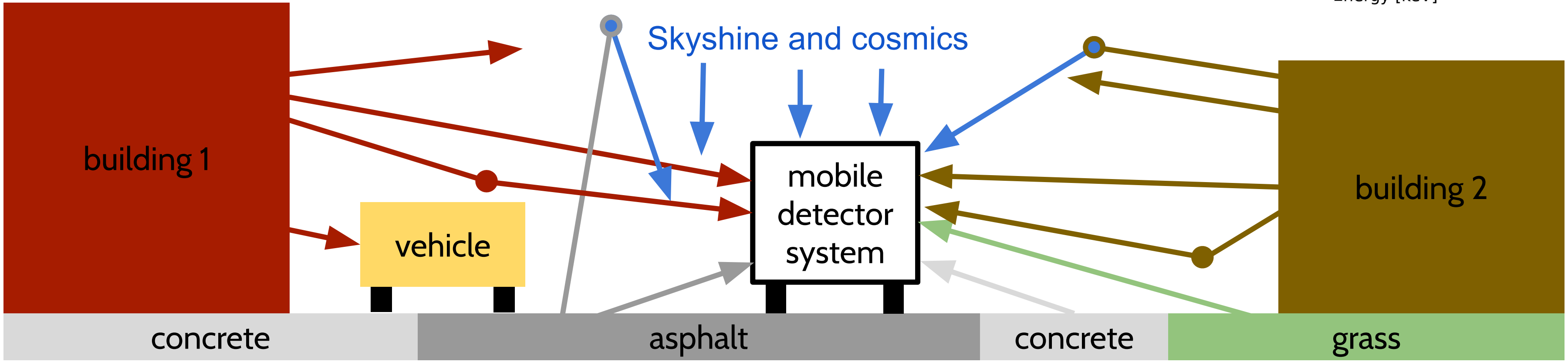

Listmode Maximum Likelihood Estimation Maximization

$$\lambda_\gamma(d,t,E'') = \sum_{(i,m)\in\mathcal{I}} \alpha_{im} \underbrace{\sum_E (S_k(E)\delta_{k\in KUT} + \delta_{k=E}) R_i^{\mathrm{3D}}(d,t,E'',E)}_{\hat{R}_{im}^{\mathrm{3D}}(d,t,E'')}$$

$$R_i^{\mathrm{3D}}(d,t,E'',E) = \sum_{E',k} A_k(d,E''|E') S_{\mathrm{air}}(E'|E, r_k(d,t)) \frac{\delta_{i,l_k(d,t)}\Delta\Omega_k}{\pi}$$

Listmode Maximum Likelihood Estimation Maximization (MLEM)

$$\alpha_{im}^{j+1} = \frac{\alpha_{im}^j}{\sum_{d,E''}\int_0^T \hat{R}_{im}^{\mathrm{3D}}(d,t,E'')\mathrm{d}t} \sum_n^N \frac{\hat{R}_{im}^{\mathrm{3D}}(d_n,t_n,E_n'')}{\sum_{(\tilde{i},\tilde{m})\in\mathcal{I}} \alpha_{\tilde{i}\tilde{m}}^j \hat{R}_{\tilde{i}\tilde{m}}^{\mathrm{3D}}(d_n,t_n,E_n'')}$$

L. Parra, H. H. Barrett, List-mode likelihood: EM algorithm and image quality estimation demonstrated on 2-D PET, IEEE Trans Med Imaging, Vol. 17, No. 2, pp. 228–235, 1998.

Results: Gross counts

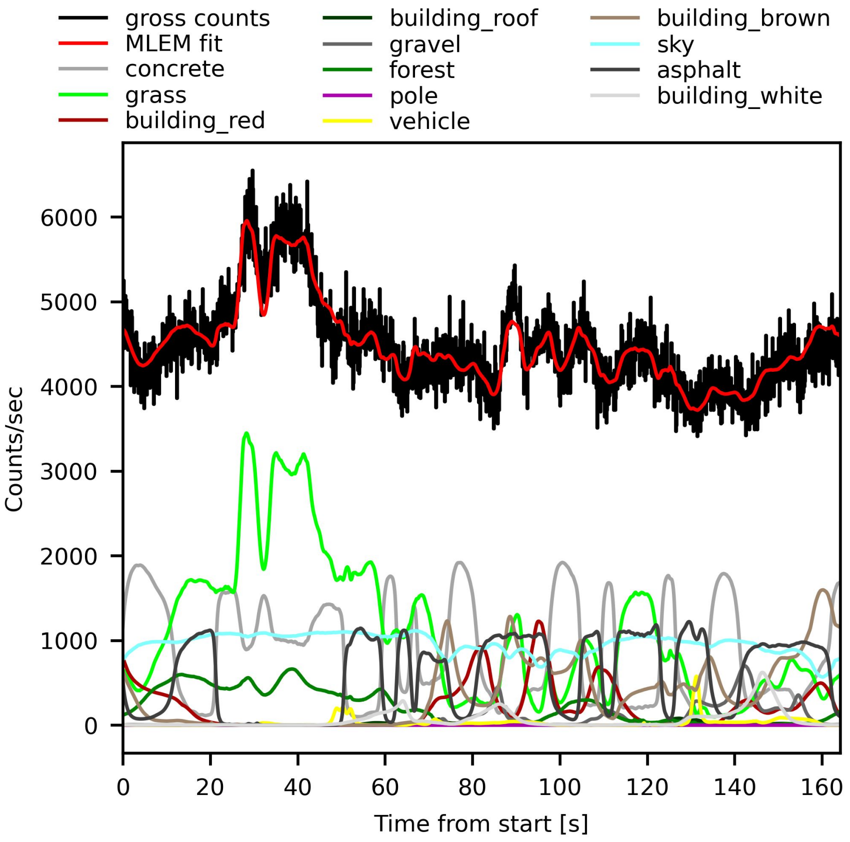

Results: KUT Activities and Sky component

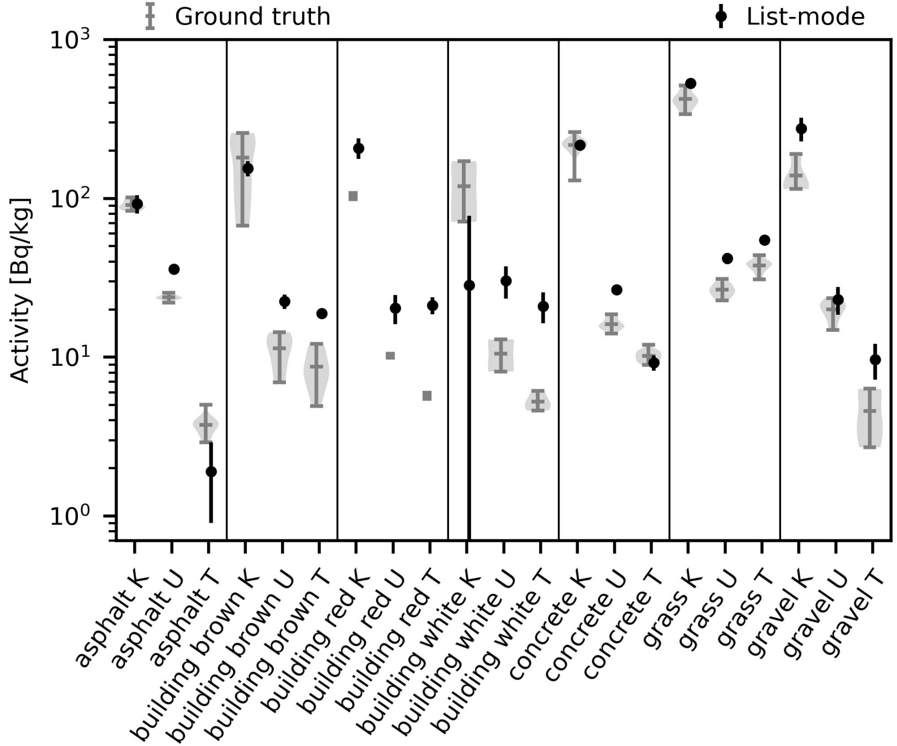

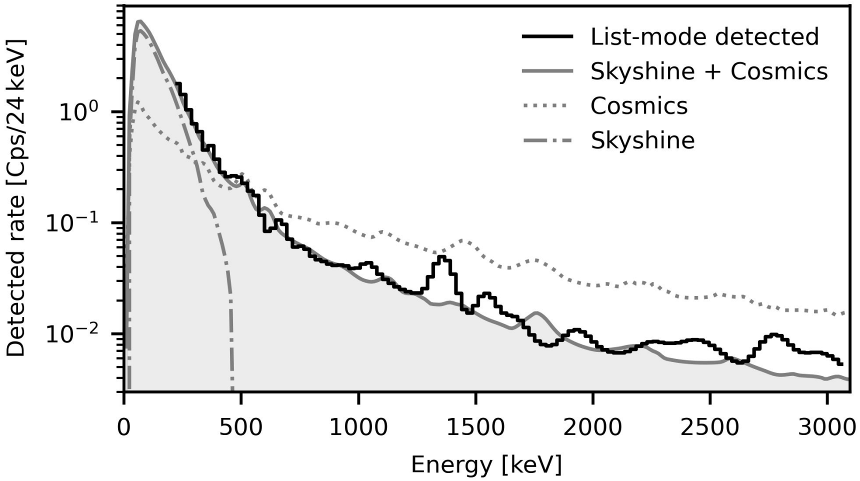

M. W. Swinney, et al., A methodology for determining the concentration of naturally occurring radioactive materials in an urban environment. Nuclear Technology, 203(3):325-335, 2018.
A. L. Mitchell, et al., Skyshine contribution to gamma ray background between 0 and 4 MeV. Technical report, Pacific Northwest National Lab. (PNNL), August 2009.
G. A. Sandness, et al., Accurate modeling of the terrestrial gamma-ray background for homeland security applications, 2009 IEEE Nuclear Science Symposium Conference Record (NSS/MIC), Orlando, FL, USA (IEEE, Piscataway, NJ, 2009), pp. 126–133.

Related Work: NMF in Oakland (Mark Bandstra)

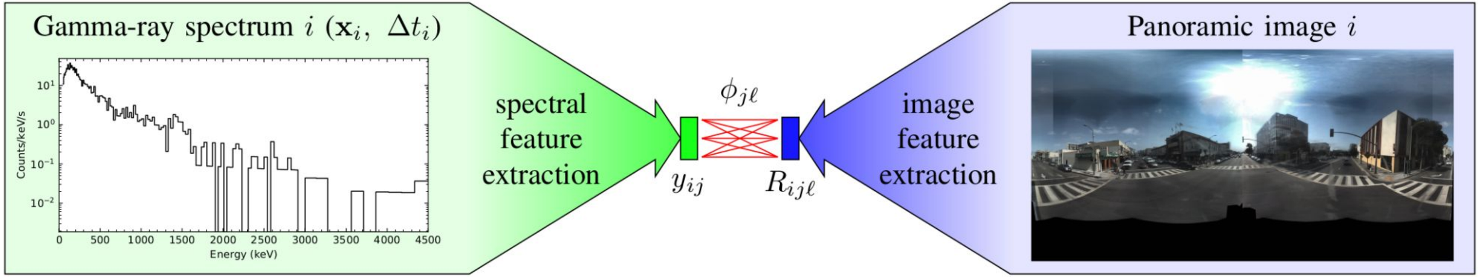

- Long (40min) continuous drive of RadMAP through Oakland, CA.
- Use various Non-negative Matrix Factorization approaches to decompose spectral data into 2-4 components
- Fit NMF weights to coverage of classes in semantically segmented video streams.

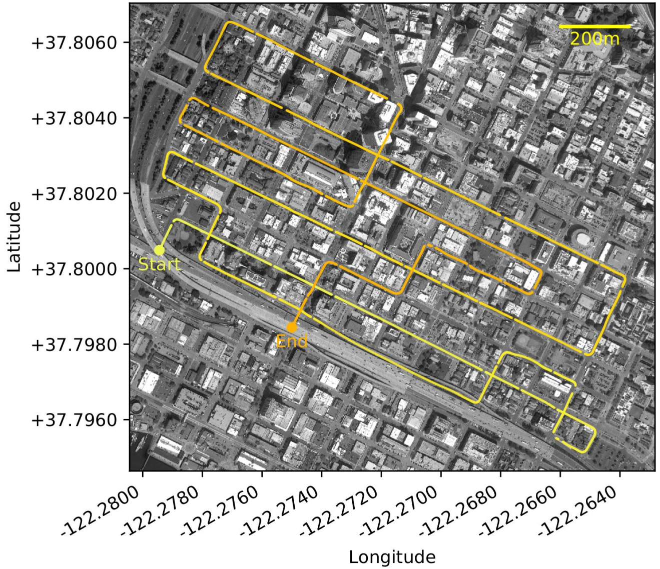

M. S. Bandstra, et al., Correlations between Panoramic Imagery and Gamma-Ray Background in an Urban Area, IEEE Transactions on Nuclear Science (submitted).

Related Work: Background "templates" for NaI calibration

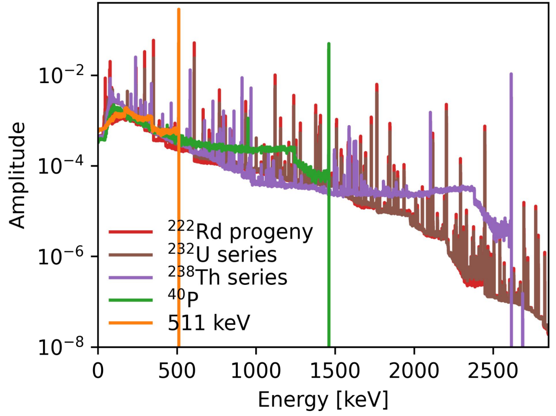

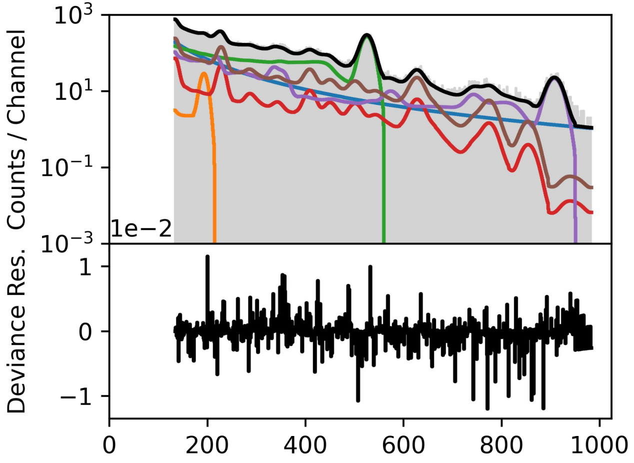

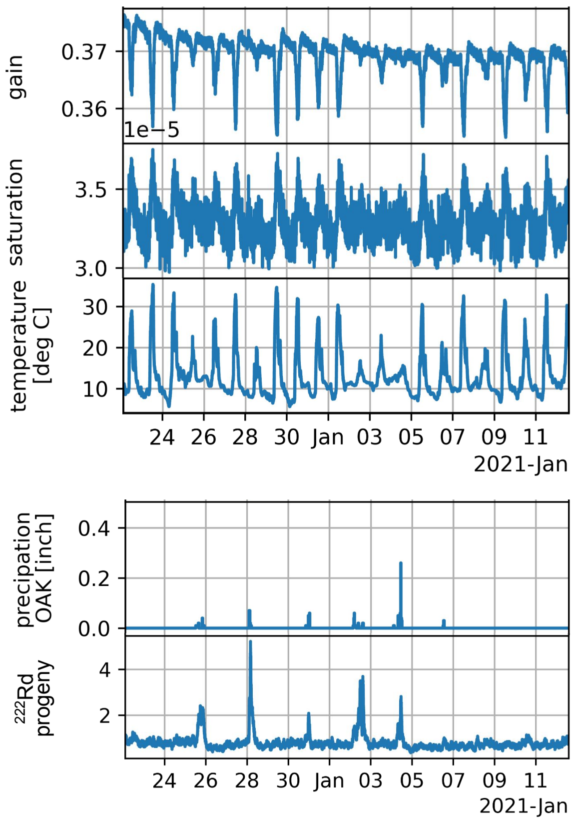

- Static sensor detector network deployed in Chicago
- Automated NaI detector calibration based on simulations of most common backgrounds and a global fit to the radiation data
- Expected correlation between calibration parameters and temperature
- Radon weight matches rain signature

Related Work: Including attenuation in source localization

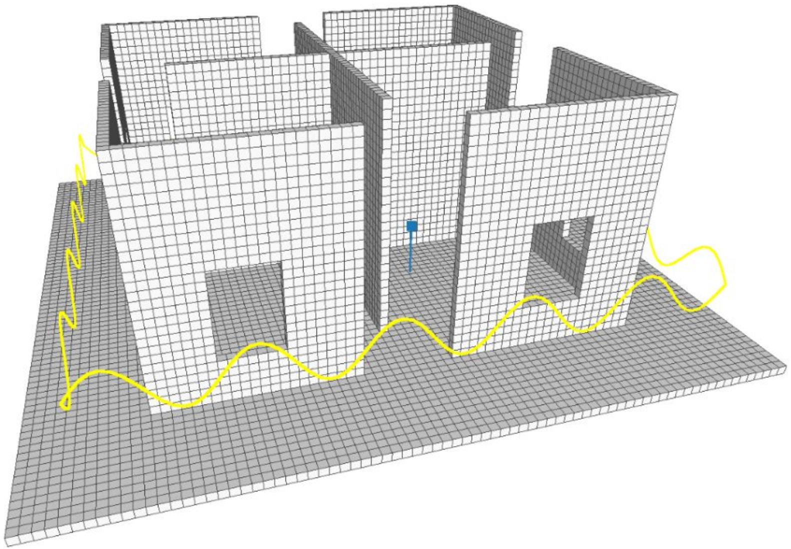

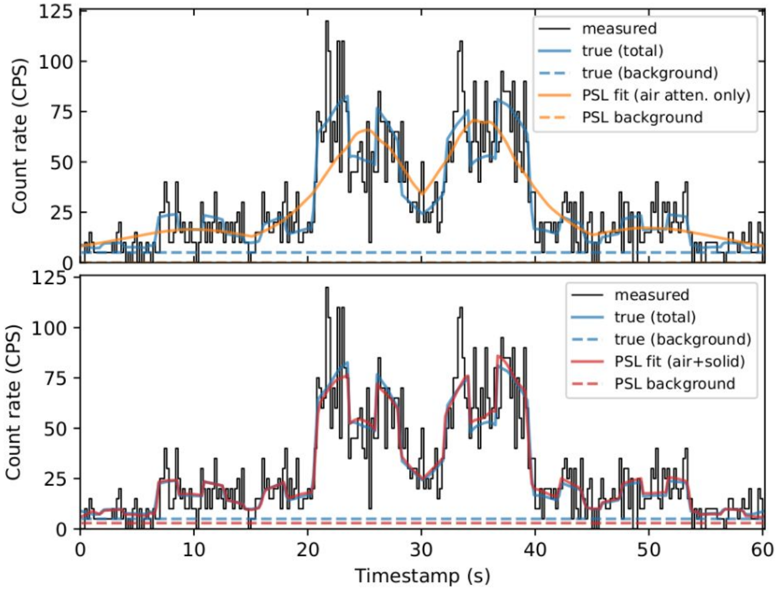

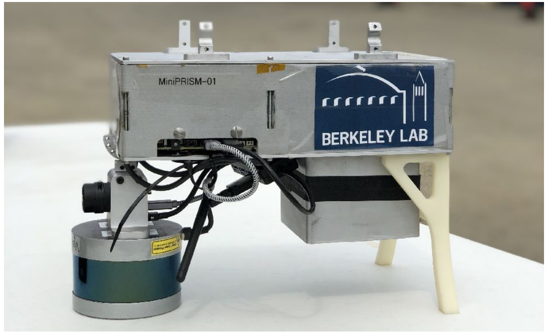

- Inclusion of occlusion and attenuation of materials in source localization
- Efforts ongoing to port algorithm to GPU to enable real-time analysis

M. S. Bandstra, et al., Improved Gamma-Ray Point Source Quantification in Three Dimensions by Modeling Attenuation in the Scene, IEEE Transactions on Nuclear Science (accepted).

BERKELEY LAB

Conclusion

- Distinct potassium-40, uranium-238 and thorium-232 activities could be derived in a short 165 second measurement based on multi-sensor data and gamma-ray transport simulations and matched to ground truth measurements in materials in a mock urban facility
- A realist representation of sky was obtained, increasing our confidence into the result.
- Searches for radioactive sources outside of regulatory control can benefit from background modeling and prediction based on contextual sensor data
- KUT modeling was used to calibrate NaI bars in static systems
- Handling of occlusion and attenuation has been used to improve source localization

Publications:

- M. Salathe, B. J. Quiter, M. S. Bandstra, J. C. Curtis, R. Meyer, and C. H.Chow, "Determining urban material activities with a vehicle-based multi-sensor system", Phys. Rev. Research 3, 023070, 2021
- M. S. Bandstra, et al., Attribution of gamma-ray background collected by a mobile detector system to its surroundings using panoramic video, NIMA 954, 161126, 2020
- M. S. Bandstra, et al., "Correlations between Panoramic Imagery and Gamma-Ray Background in an Urban Area", 2019 IEEE Nuclear Science Symposium and Medical Imaging Conference (2019), pp. 1–5
- M. Salathe, et al., "Using 3D-Scene Data from a Mobile Detector System to Model Gamma-Ray Backgrounds", 2019 IEEE Nuclear Science Symposium and Medical Imaging Conference (2019), pp. 1–4

BERKELEY LAB

Thanks / Questions

Marco Salathe
msalathe@lbl.gov

Contributors (Main topic)
- Brian J. Quiter
- Mark S. Bandstra
- Joseph C. Curtis

Data collection (Main topic)
- Ross Meyer
- Chun Ho Chow

Related work
- Basically everybody in the Applied Nuclear Program

Acknowledgments
- This work was performed under the auspices of the US Department of Energy by Lawrence Berkeley National Laboratory under Contract DE-AC02-05CH11231.
- The project was funded by the US Department of Energy, National Nuclear Security Administration, Office of Defense Nuclear Nonproliferation Research and Development (DNN R&D).
- This research used resources of the National Energy Research Scientific Computing Center (NERSC), a U.S. Department of Energy Office of Science User Facility operated under Contract No. DE-AC02-05CH11231.

Uncertainty estimation

$$\lambda_\gamma(d,t,E'') = \sum_{(i,m)\in\mathcal{I}} \alpha_{im} \underbrace{\sum_E (S_k(E)\delta_{k\in KUT} + \delta_{k=E}) R_i^{3\mathrm{D}}(d,t,E'',E)}_{\hat{R}_{im}^{3\mathrm{D}}(d,t,E'')}$$

- Non-negativity due to Poisson nature of problem
- Some activities and sky bins are close to zero

Gaussian statistics not applicable and the Fisher information and the Cramér-Rao inequality not valid for uncertainty estimation.

- Monte-Carlo simulations (5000 samples):
  - Use MLEM solution to calculate count-rate estimate
  - Randomly sample from Poisson distribution
  - Calculate MLEM solution for sampled result
- Sample variance ⇒ uncertainty estimation
- Sample covariance ⇒ covariance/correlation matrix

- Use histogram MLEM[1] for reduced random-access memory usage and computations and simple Poisson sampling:
  - Single detector placed at center of array
  - Combining counts
  - Summing effective area

Histogram Maximum Likelihood Estimation Method MLEM

$$\alpha_{im}^{j+1} = \frac{\alpha_{im}^{j}}{\sum_{t,E'} \hat{R}_{im}^{3\mathrm{D}}(t,E'')} \sum_{t,E''} \frac{n(t,E'')\hat{R}_{im}^{3\mathrm{D}}(t,E'')}{\sum_{\tilde{i},\tilde{m}} \alpha_{\tilde{i}\tilde{m}}^{j} \hat{R}_{\tilde{i}\tilde{m}}^{3\mathrm{D}}(t,E'')}$$

L. A. Shepp, Y. Vardi, Maximum Likelihood Reconstruction for Emission Tomography, IEEE Trans. Med. Imaging. Vol. 1, No. 2, pp. 113-122, 1982.

- We considered Listmode and Histogram mode similar enough for this approximation to be sufficient.

Correlation Matrix

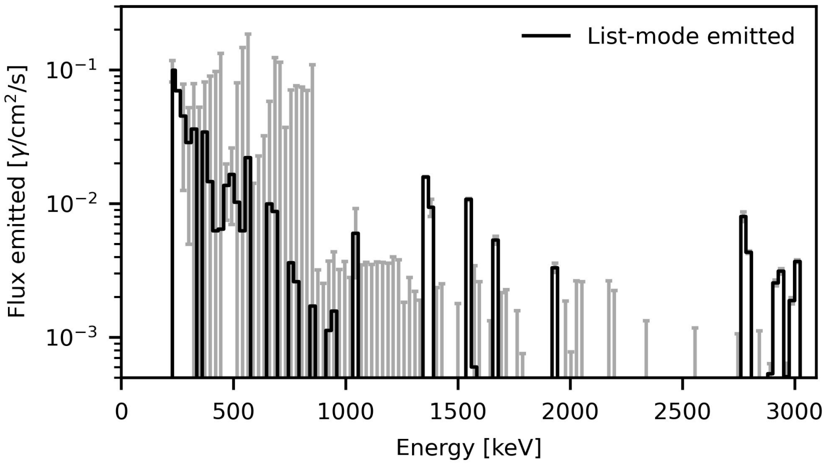

Correlation Matrix derived from covariance matrix, normalized with uncertainties

$$\mathrm{corr}(\mathbf{X}) = \left(\mathrm{diag}(\mathrm{cov}(\mathbf{X}))\right)^{-\frac{1}{2}}\ \mathrm{cov}(\mathbf{X})\ \left(\mathrm{diag}(\mathrm{cov}(\mathbf{X}))\right)^{-\frac{1}{2}}$$

X being a random vector

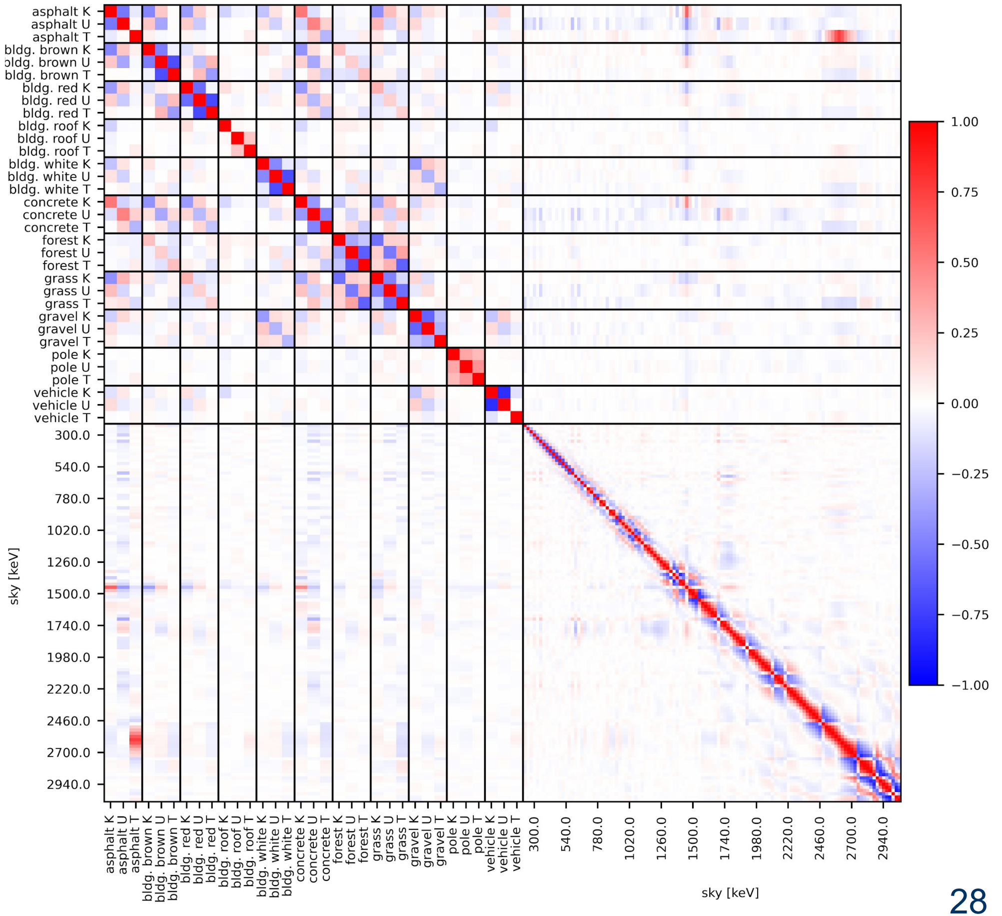

BERKELEY LAB

Correlation Matrix

- Different isotopes but same label are anti-correlate
  ⇒ total flux more confined than individual activities
  - Labels Building roof, and Poles are poorly constrained and don't show this behavior
- Correlations between labels seen at different times:
  - Asphalt/Concrete, Building brown/Forest, Building red/Grass
- Anti-correlations between labels seen at the same time:
  - Forest/Grass, Concrete/Grass, Asphalt/Grass, Building brown and red/Concrete, Building white/Gravel
- Anti-correlation between K, T and sky, correlation between U and sky and an anti-correlation band around 1.8MeV within sky
  ⇒ balance between terrestrial uranium and radon in sky

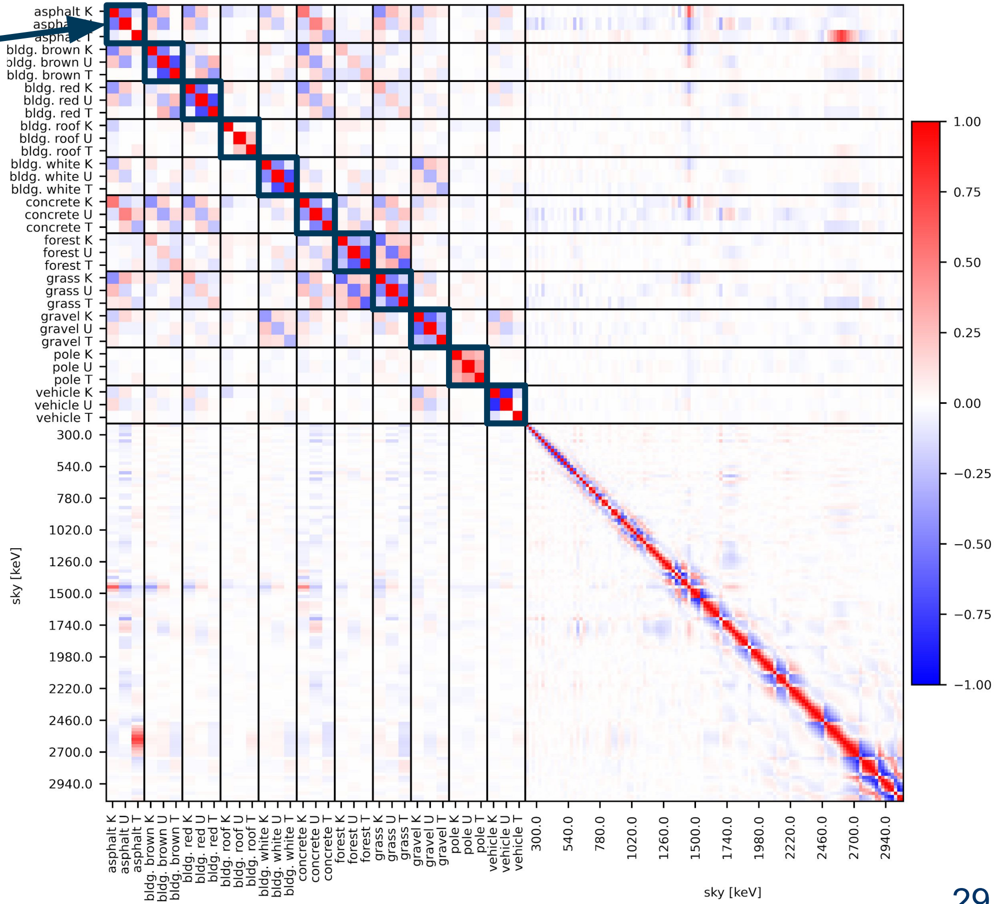

Correlation Matrix

- Different isotopes but same label are anti-correlate
  ⇒ total flux more confined than individual activities
  - Labels Building roof, and Poles are poorly constrained and don't show this behavior
- Correlations between labels seen at different times:
  - Asphalt/Concrete, Building brown/Forest, Building red/Grass
- Anti-correlations between labels seen at the same time:
  - Forest/Grass, Concrete/Grass, Asphalt/Grass, Building brown and red/Concrete, Building white/Gravel
- Anti-correlation between K, T and sky, correlation between U and sky and an anti-correlation band around 1.8MeV within sky
  ⇒ balance between terrestrial uranium and radon in sky

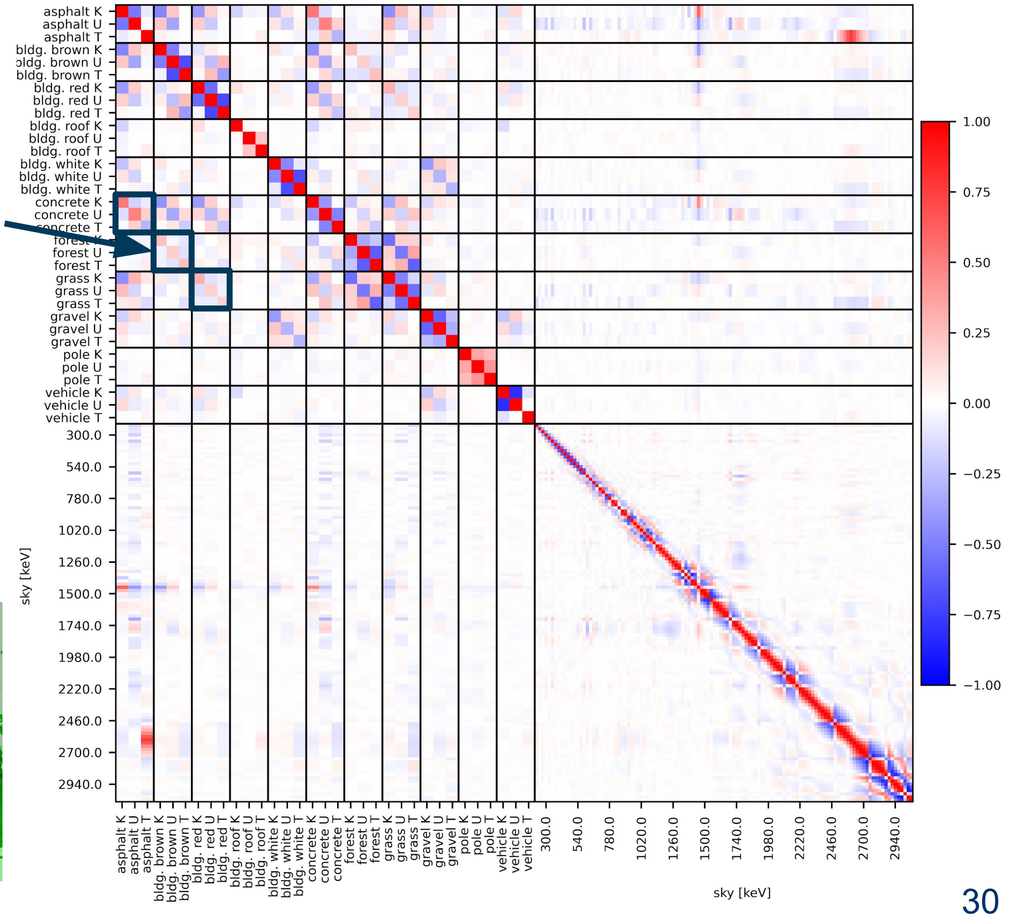

Correlation Matrix

- Different isotopes but same label are anti-correlate
  ⇒ total flux more confined than individual activities
  - Labels Building roof, and Poles are poorly constrained and don't show this behavior
- Correlations between labels seen at different times:
  - Asphalt/Concrete, Building brown/Forest, Building red/Grass
- Anti-correlations between labels seen at the same time:
  - Forest/Grass, Concrete/Grass, Asphalt/Grass, Building brown and red/Concrete, Building white/Gravel
- Anti-correlation between K, T and sky, correlation between U and sky and an anti-correlation band around 1.8MeV within sky
  ⇒ balance between terrestrial uranium and radon in sky

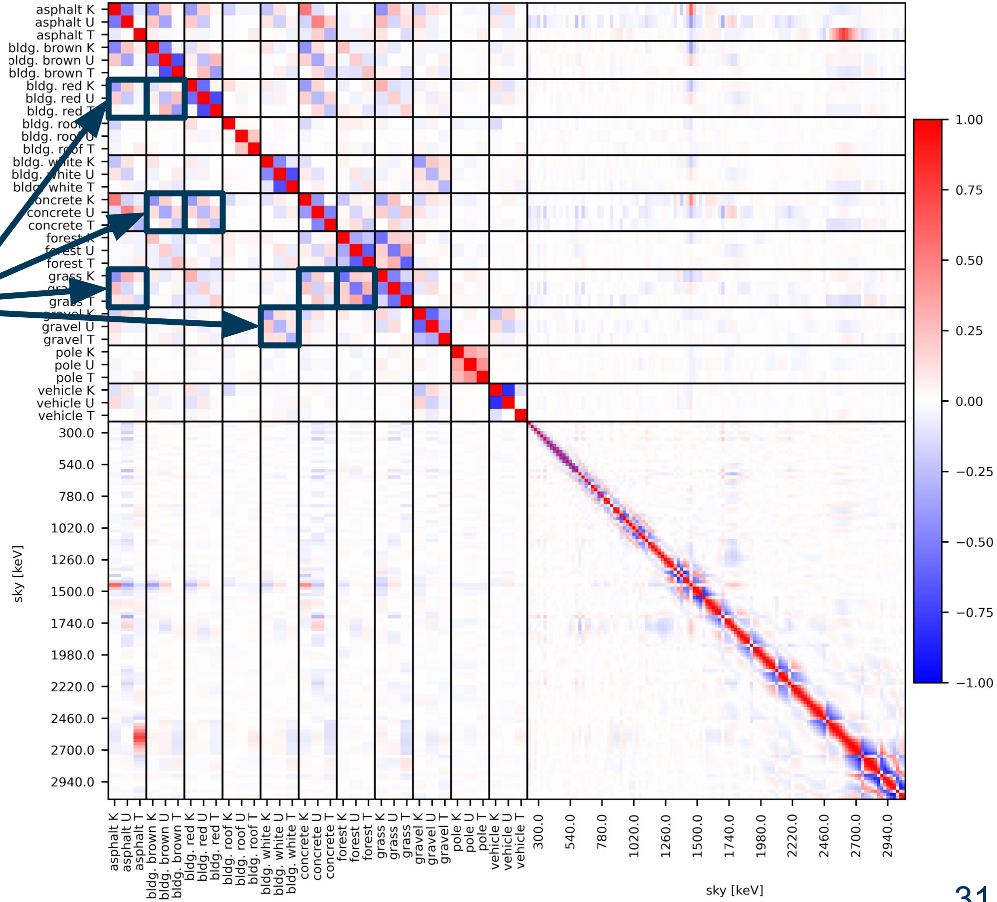

Correlation Matrix

BERKELEY LAB

- Different isotopes but same label are anti-correlate
  ⇒ total flux more confined than individual activities
  - Labels Building roof, and Poles are poorly constrained and don't show this behavior
- Correlations between labels seen at different times:
  - Asphalt/Concrete, Building brown/Forest, Building red/Grass
- Anti-correlations between labels seen at the same time:
  - Forest/Grass, Concrete/Grass, Asphalt/Grass, Building brown and red/Concrete, Building white/Gravel
- Anti-correlation between K, T and sky, correlation between U and sky and an anti-correlation band around 1.8MeV within sky
  ⇒ balance between terrestrial uranium and radon in sky

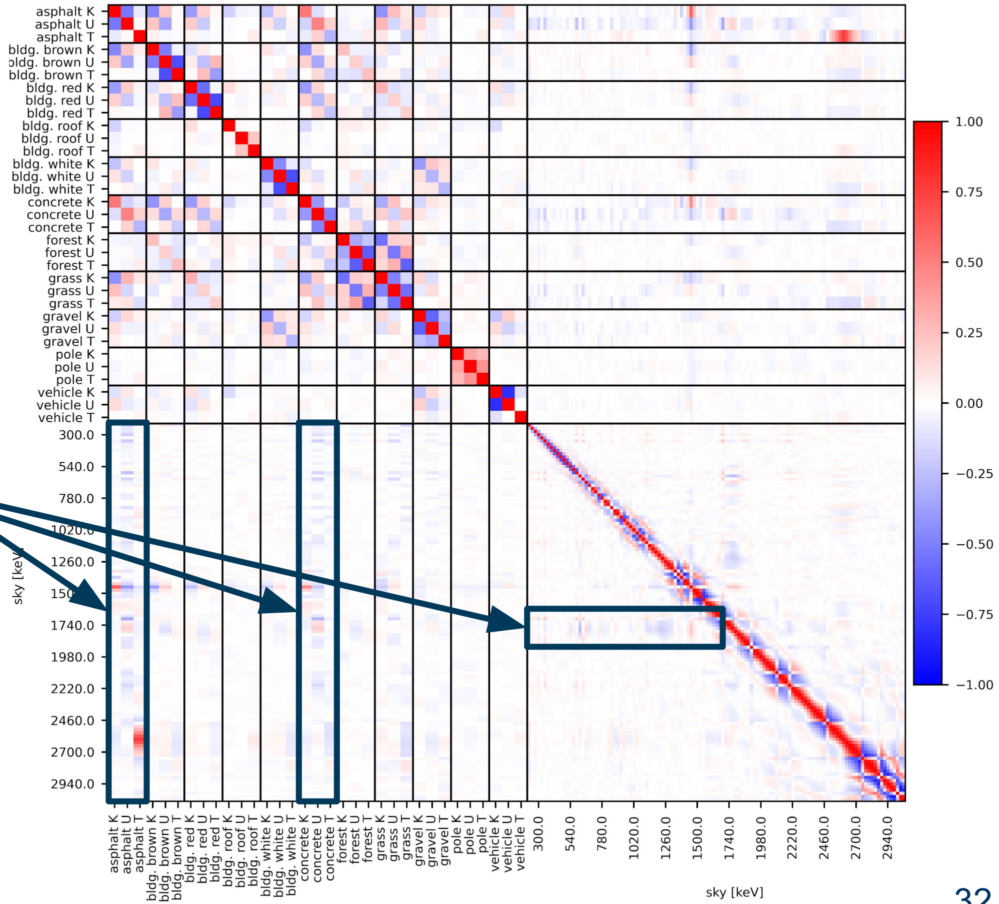

Analysis pipeline

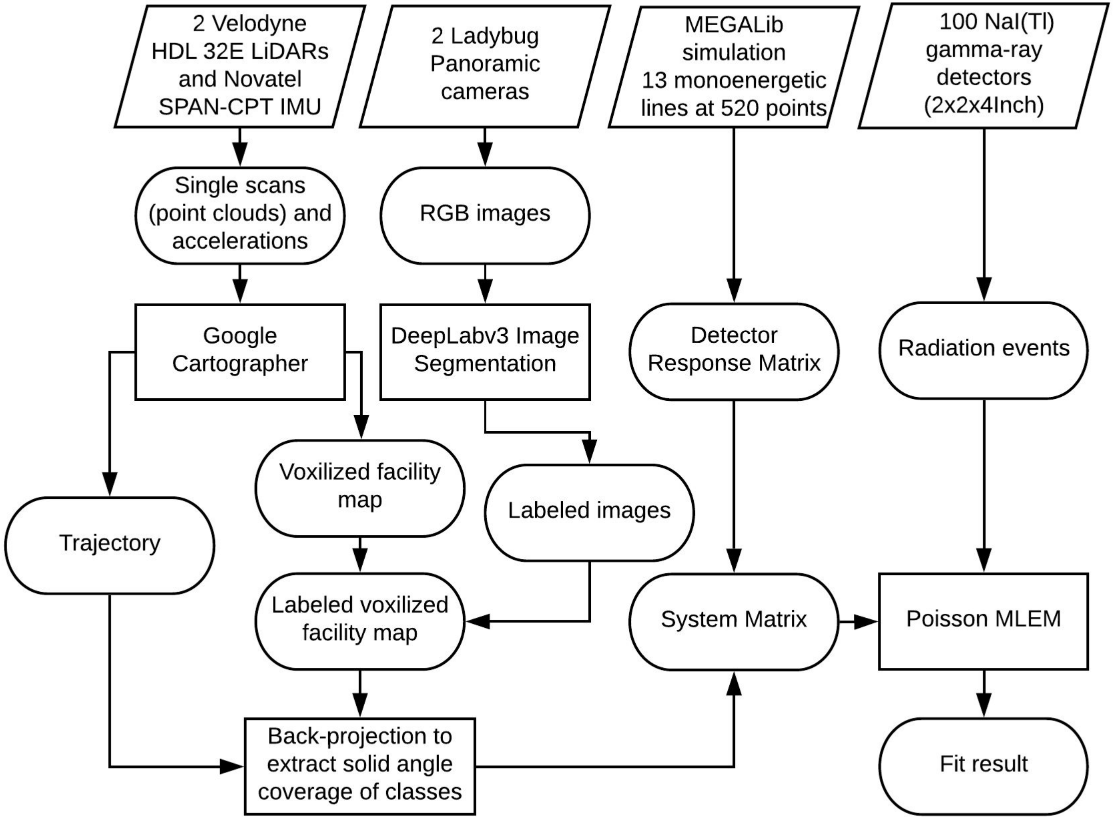

Net flux by labels

Class	Ground truth [γ/s/cm²]	Camera only[1] [γ/s/cm²]	LiDAR no energy threshold [γ/s/cm²]	LiDAR with energy threshold [γ/s/cm²]
Vehicle	N/A	1.30 ± 0.14	1.77	1.38
Grass	2.462	2.25 ± 0.05	3.66	3.59
Building roof	N/A	0.00 ± 0.31	2.19	1.34
Sky	N/A	0.54 ± 0.03	0.53	0.61
Forest	N/A	0.93 ± 0.05	4.59	1.80
Concrete	0.985	1.05 ± 0.05	1.57	1.18
Building red	0.397	1.18 ± 0.03	1.36	1.54
Asphalt	0.836	0.72 ± 0.10	1.39	1.00
Building white	0.311 / 0.501	1.00 ± 0.05	2.08	1.49
Building brown	0.446 / 0.658	1.02 ± 0.03	1.48	1.39
Gravel	0.831	1.08 ± 0.06	2.67	1.46

- Close to ground truth and camera only for most labels
- Energy threshold was set at 216keV and resulting flux were divided by fraction of events in ground truth above threshold
- Energy threshold reduces most of the fluxes to agree better with ground truth

Good agreement of a 2 minute measurement with a month long measurement campaign

[1]*M. S. Bandstra, et. al., Attribution of gamma-ray background collected by a mobile detector system to its surroundings using panoramic video, NIMA, 2018.*

Results: Full spectral fit vs spectral templates approach

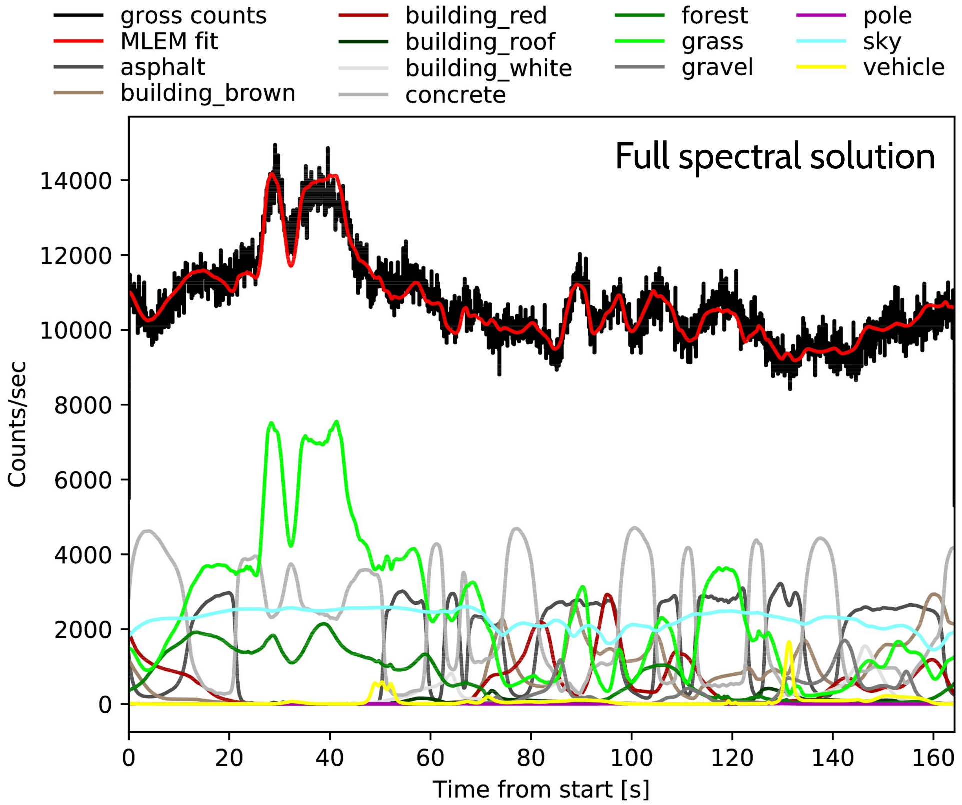

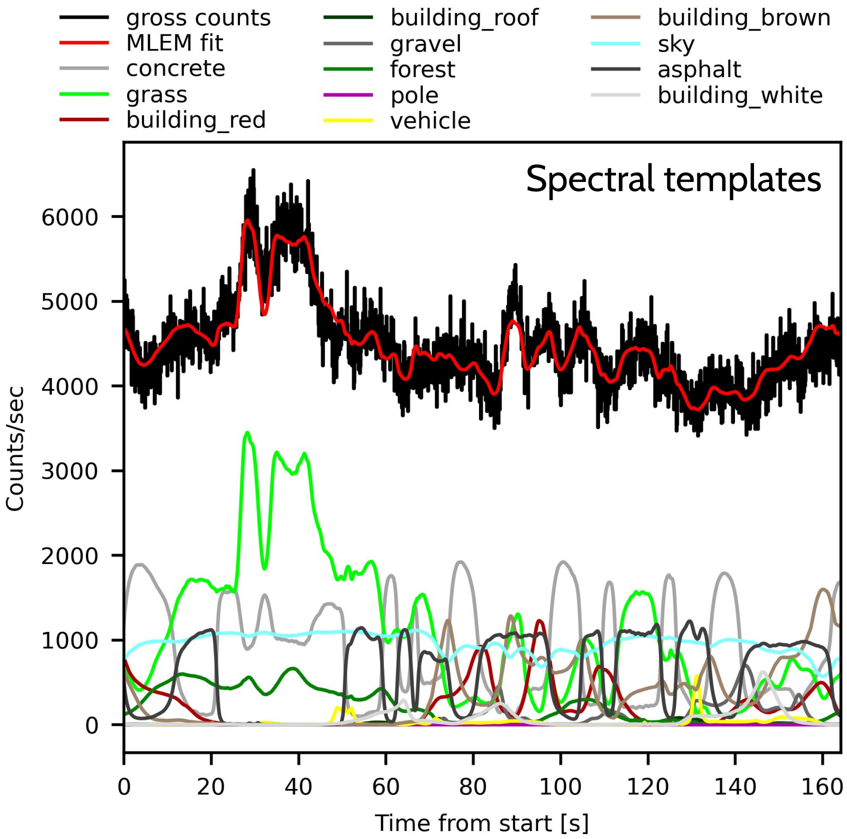

Results: Full spectral inversion

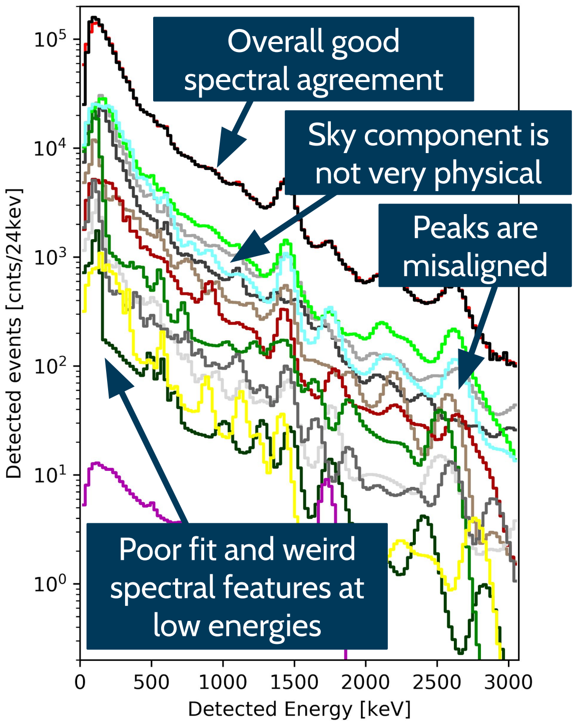

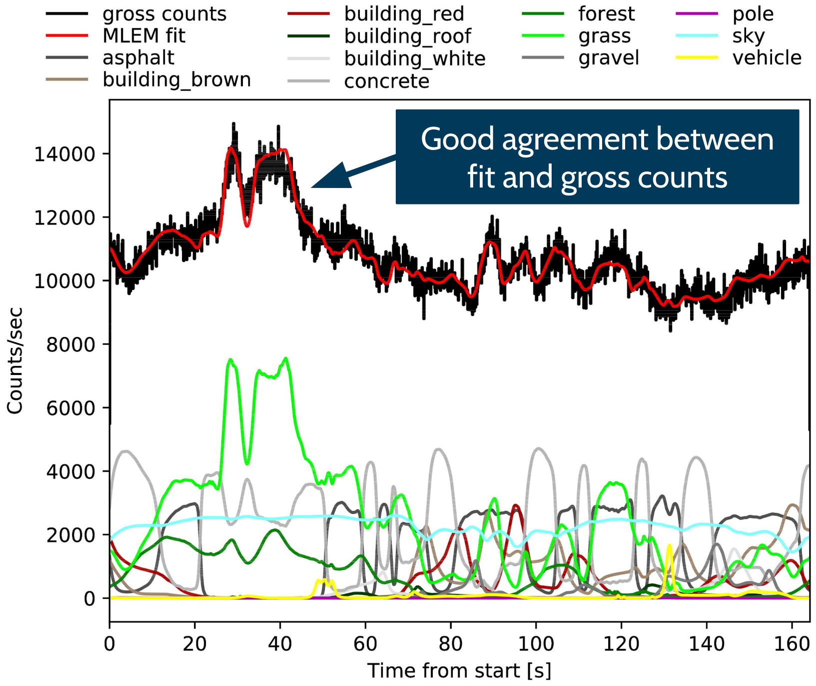

Modeling Gamma-ray backgrounds

Average number of observed photon in detector *d* at time *t* at energy *E''*

Energy dependent net flux emitted by label *i* in the scene

Effective area (detector efficiency and response) of impending gamma rays of *E'*

Down scattering and attenuation of gamma rays emitted at *E*

Distance of a solid angle element (pixel)

Label of a solid angle element (pixel)

Size of solid angle element *k* (pixel)

$$\lambda_\gamma(d,t,E'') = \sum_{i,E} f_i(E) \underbrace{\sum_{E',k} A_k(d,E''|E')\, S_{\mathrm{air}}(E'|E, r_k(d,t))\, \frac{\delta_{i,l_k(d,t)}\,\Delta\Omega_k}{\pi}}_{R_i^{\mathrm{3D}}(d,t,E'',E)}$$

System response

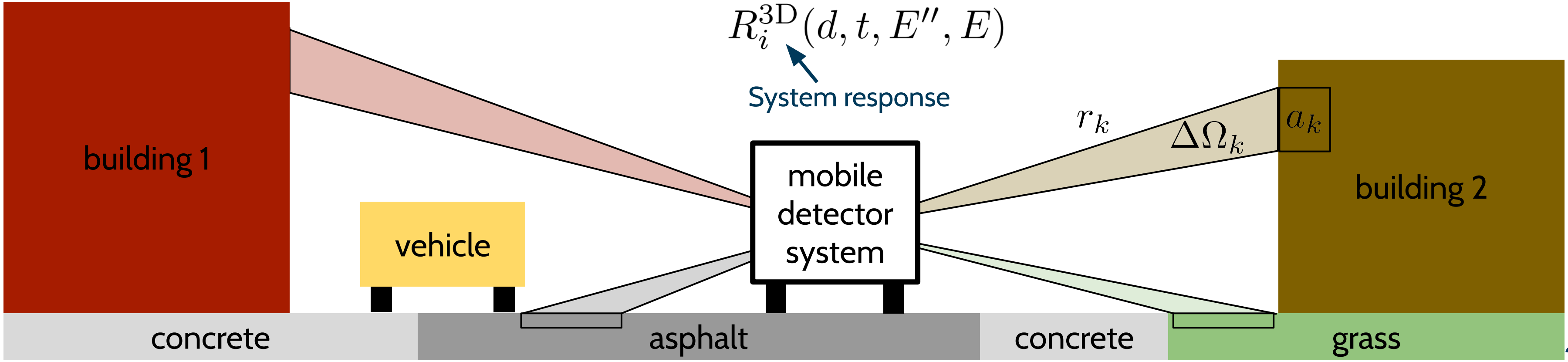

Modeling Gamma-ray backgrounds

All quantities including energies are discrete
i = 12 labels
E, E', E" = 127 energies (0 - 3072keV)
k = 300x600 pixels
d = 100 detector modules
t = 1650 time steps (0 - 165sec)
r = 256 distances (0 - 80m)

Simulation of gamma-ray transport in materials and through air (see last years talk and conference proceedings)
M. Salathe, et al., "Using 3D-Scene Data from a Mobile Detector System to Model Gamma-Ray Backgrounds," *2019 IEEE Nuclear Science Symposium and Medical Imaging Conference (NSS/MIC)*, Manchester, United Kingdom, 2019, pp. 1-4.

Based on contextual data from mobile system, producing a 3D segmented representation of the facility (refresher later)

Divide field of view of detectors into solid angle elements (pixels)

$$\lambda_\gamma(d,t,E'') = \sum_{i,E} f_i(E) \underbrace{\sum_{E',k} A_k(d,E''|E')\, S_{\mathrm{air}}(E'|E,r_k(d,t))\, \frac{\delta_{i,l_k(d,t)}\,\Delta\Omega_k}{\pi}}_{R_i^{3\mathrm{D}}(d,t,E'',E)}$$

~1500 free parameters!

Large multi-dimensional tensor!

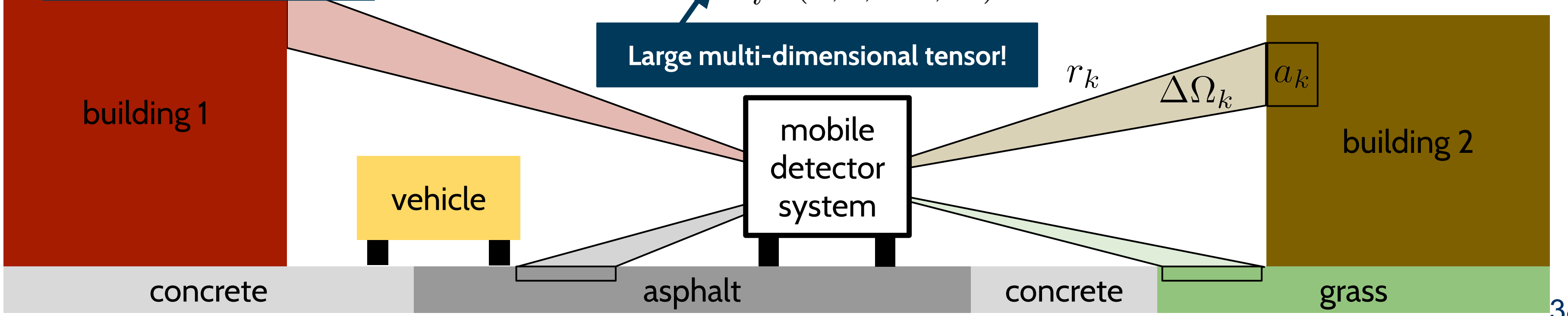

Modeling Gamma-ray backgrounds

Main sources of NORM:

- Terrestrial — K-40, U-238 series, Th-232 series (KUT)
- Airborne — radon, skyshine
- Cosmic — continuum, 511 keV from positrons

$$\lambda_\gamma(d,t,E'') = \boxed{\sum_{i,E} f_i(E)} R_i^{3\mathrm{D}}(d,t,E'',E)$$

Precalculated with gamma-ray transport simulations of thick (2m) slab made up of soil.

$$\sum_{i,E} f_i(E) = \sum_{\boxed{(i,m)\in\mathcal{I}}} \alpha_{im} \sum_E (S_k(E)\delta_{k\in KUT} + \delta_{k=E}).$$

119 energy bins between 216keV and 3072keV, all unconstrained

$$\mathcal{I} = \{(i,m) : i \neq \text{sky}, m \in \{K,U,T\} \text{ or } \quad i = \text{sky}, m \in \{E_1, ..., E_N\}\}$$

$$\lambda_\gamma(d,t,E'') = \sum_{(i,m)\in\mathcal{I}} \alpha_{im} \underbrace{\sum_E (S_k(E)\delta_{k\in KUT} + \delta_{k=E}) R_i^{3\mathrm{D}}(d,t,E'',E)}_{\hat{R}_{im}^{3\mathrm{D}}(d,t,E'')}$$

Linear system to be solved with MLEM

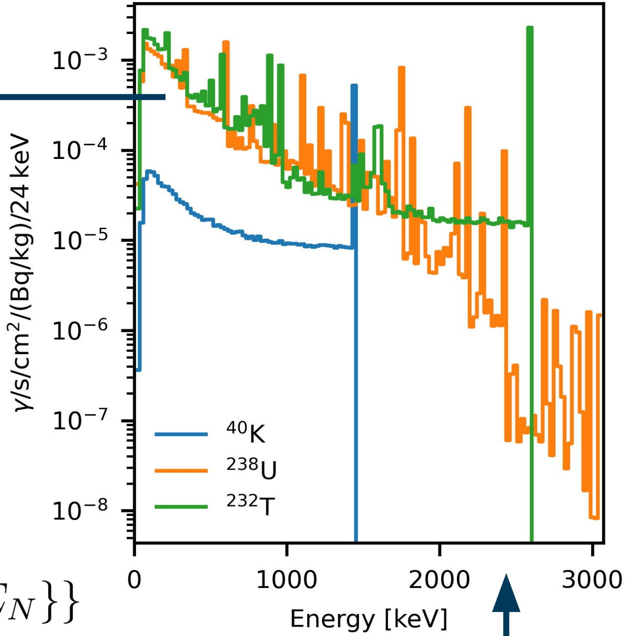

Normalized to represent activity of isotopes